

# New Hyperbranched Conjugated Polymers Containing Hexaphenylbenzene and Oxadiazole Units: Convenient Synthesis and Efficient Deep Blue Emitters for PLEDs Application

Zhong'an Li,<sup>†</sup> Shanghai Ye,<sup>‡</sup> Yunqi Liu,<sup>\*,‡</sup> Gu Yu,<sup>‡</sup> Wenbo Wu,<sup>†</sup> Jingui Qin,<sup>†</sup> and Zhen Li<sup>\*,†</sup>

Department of Chemistry, Hubei Key Lab on Organic and Polymeric Opto-Electronic Materials, Wuhan University, Wuhan 430072, China, and Organic Solids Laboratories, Institute of Chemistry, The Chinese Academy of Sciences, Beijing 100080, China

Received: February 15, 2010; Revised Manuscript Received: May 31, 2010

In this article, four “A<sub>3</sub>+B<sub>2</sub>+C<sub>2</sub>”-type hyperbranched conjugated polymers (**P1–P4**) containing hexaphenylbenzene as the core were synthesized successfully for the first time with high yields through one-pot Suzuki polymerization reaction. The copolymerization percent of 1,3,4-oxadiazole units was adjusted to investigate the effect of polymer composition on the physical, optical, and EL properties. All polymers were well-characterized and exhibited good solubility, film-forming ability, and thermal stability. Both the solution and the films of these hyperbranched polymers emitted pure and stable deep-blue light emission, and their PL spectra did not change after annealing at 150 °C for 0.5 h in air, indicating that the hyperbranched structure, coupled to the introduced hexaphenylbenzene moieties, effectively suppressed the formation of aggregation excimer and keto defects. Two-layer PLED devices were fabricated to investigate the electroluminescence properties of these hyperbranched polymers, and **P3** demonstrated a maximum luminance efficiency of 0.72 cd/A and a maximum brightness of 549 cd/m<sup>2</sup> at 16.5 V.

## Introduction

Conjugated polymers have extensively attracted interest for their potential applications in flat-panel displays.<sup>1–5</sup> In the research field of polymer light-emitting diodes (PLEDs), among the three primary color (red, green, and blue) light-emitting materials required for full color displays, the biggest challenge so far has been to obtain efficient and spectra-stable blue light-emitting polymers, which could be easily converted to green or red light with proper doped dyes.<sup>6</sup> Various kinds of blue-light conjugated polymers have been proposed, and the most promising materials were polyfluorene (PF) and their derivatives because of their high photoluminescence (PL) and EL efficiency as well as easy tunability of physical properties through the chemical structure modification and copolymerization.<sup>7–12</sup> However, the notorious long-wavelength emission owing to the formation of ketone defects or excimers/aggregation in the condensed state hampered PFs as excellent blue emitters.<sup>13–18</sup> In the past decades, the construction of dendritic blue light-emitting materials has been demonstrated as an effective method to solve the above problem because their highly branched and globular molecular structure could favor exciton confinement and decrease intra- and interchain exciton annihilation, which thereby significantly improved EL efficiency and thermal stability and made the materials form good quality amorphous films.<sup>19–25</sup> Compared with dendrimers,<sup>26–28</sup> hyperbranched polymers exhibited comparable properties but could be prepared very easily just through one-pot, single-step reaction procedures. This was the main reason why fluorene-based hyperbranched polymers have received considerable attention of synthetic chemists.<sup>29–38</sup>

Hexaphenylbenzene, with the diameter as 1.14 nm, was an important and thoroughly investigated organic chromophore because of its 2D structure: the hexagonal symmetry of benzene, which could be seen as the model compound of dendritic PPPs, another kind of important blue-emitting conjugated polymers.<sup>39</sup> Its derivatives, also termed as Müllen's dendrimers, were both shape-persistent and chemically stable. In particular, its 3D shielding ability could hinder aggregate formation in the solid state much more efficiently than the Frechét type of dendrons and thereby increase the color stability and quantum efficiency of the devices, as demonstrated by some PFs and PPVs bearing the Müllen's dendrimer block in the side-chains.<sup>40–43</sup> However, so far, hyperbranched PFs based on hexaphenylbenzene moieties have not been reported in the literature, possibly because of the synthetic difficulty,<sup>39–43</sup> although these polymers were expected to exhibit the merits of both hyperbranched polymers and Müllen's dendrimers to achieve much better comprehensive performance of devices.

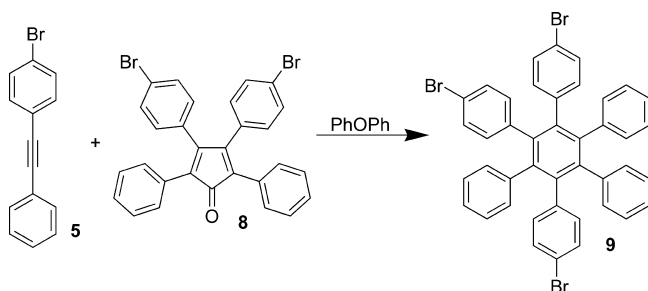
In general, to improve the EL efficiency, it was critical to achieve both efficient charge injection and balanced mobility of both charge carriers inside the electroluminescent polymers.<sup>44,45</sup> The introduction of nitrogen-containing heterocyclo-rings<sup>46</sup> such as 1,3,4-oxadiazole,<sup>47–49</sup> pyridine,<sup>50</sup> thiazole,<sup>51</sup> triazole,<sup>52</sup> triazine,<sup>52</sup> benzothiadiazole units,<sup>53</sup> and so on into the conjugated polymers has been proven as an alternative method to achieve the balance of charge transport. Among the used nitrogen-containing heterocyclo-rings, 1,3,4-oxadiazole derivatives were the famous electron-deficient materials with good thermal and chemical stabilities as well as high PL quantum yields and generally were used as electron-transport materials in PLEDs.<sup>46–49</sup> To date, 1,3,4-oxadiazole moieties have been widely utilized to construct small molecules and linear polymers; however, their application in hyperbranched polymers was still scarce.<sup>54,55</sup> Therefore, in this article, for the first time, we successfully synthesized a new “A<sub>3</sub>+B<sub>2</sub>”-type blue-emitting hyperbranched conjugated polyfluorene (**P1**) using 1,2,4-tribromohexaphenyl-

\* Corresponding authors. Tel: 86-27-62254108. Fax: 86-27-68756757. E-mail: lizhen@whu.edu.cn (Z.L.) and liuyq@iccas.ac.cn (Y.L.).

<sup>†</sup> Wuhan University.

<sup>‡</sup> The Chinese Academy of Sciences.

## SCHEME 1



benzene (**9**) as the core (Schemes 1 and 2) by controlling the reaction time to avoid gelation of the hyperbranched polymers. Also, to improve further the EL efficiency of **P1**, we used 2,5-bis(4-bromophenyl)-1,3,4-oxadiazole as linear copolymerization units to afford other three hyperbranched polyfluorenes **P2–P4** (Scheme 2). The PLED devices have been fabricated based on **P1–P4** and demonstrated pure and stable deep blue light emission centered at  $\sim 420$  nm (fwhm = 40 nm) and improved EL efficiency (0.72 cd/A of **P3**).

## Results and Discussion

**Synthesis and Structural Characterization.** As shown in Scheme 1 and Scheme S1 of the Supporting Information, monomer 2,5-bis(4-bromophenyl)-1,3,4-oxadiazole (**2**) was easily synthesized,<sup>48</sup> whereas 1,2,4-tribromohexaphenylbenzene (**9**) has not been reported, which was prepared through a Diels–Alder reaction of compound **5** with **8** in the yield of 85.8%, similar to the literature work.<sup>56</sup> The synthetic route of polymers **P1–P4** is shown in Scheme 2, and the polymerization procedure was proceeded smoothly through the Suzuki coupling reaction using  $\text{Pd}(\text{PPh}_3)_4$  as a catalyst,  $\text{Na}_2\text{CO}_3$  as a base, and a mixture of THF/ $\text{H}_2\text{O}$  (4/1, v/v) as the solvent. Our previous studies showed that copolymerization of **A2** and **B3** or **B4** monomers might lead to the formation of gelation rapidly.<sup>57,58</sup> Many reaction conditions could affect the final products in the **A2** and **B3** polymerization, such as temperature, time, concentrations and molar ratio of the monomers, and solvents.<sup>54</sup> To avoid the possible formation of gelation, the concentration of **10** was fixed at 0.025 mol/L, and different reaction time (Table 1) was controlled before end-capped groups (phenylboronic acid and bromobenzene) were added to react with the bromo- and boronic ester end groups, which might quench the fluorescence of the resultant hyperbranched polymers. Also, the molar ratios of the starting materials (**2**, **9**, **10**), as shown in Scheme 2, were adjusted to investigate the effect of the polymer composition on the

## SCHEME 2

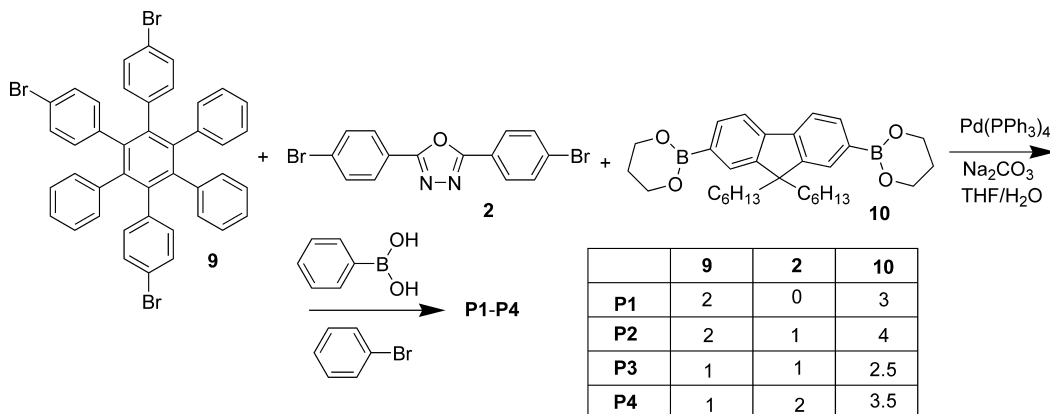
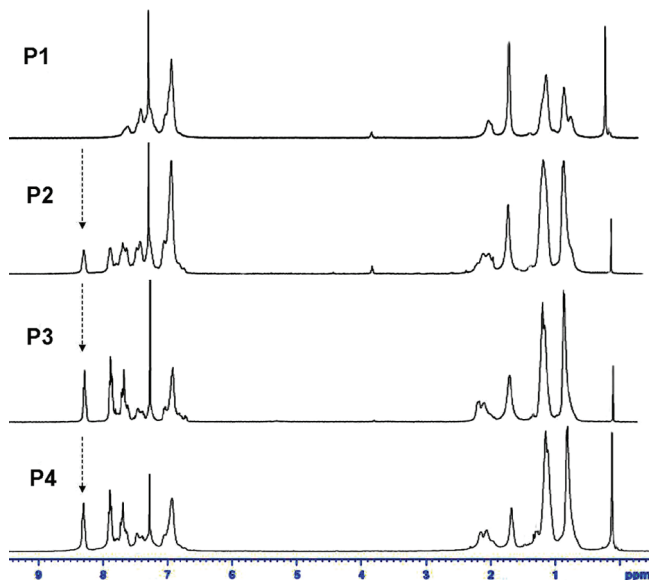


TABLE 1: Polymerization Results of Hyperbranched Polymers

no.	reaction		$M_w \times 10^{4b}$	$M_w/M_n^b$	$T_g$ (°C) <sup>c</sup>	$T_d$ (°C) <sup>d</sup>
	time (h) <sup>a</sup>	yield (%)				
<b>P1</b>	12	63.1	1.25	1.70	182	364
<b>P2</b>	20	69.3	3.21	2.35	155	312
<b>P3</b>	28	70.9	1.25	1.42	191	347
<b>P4</b>	21	80.7	2.03	3.05	180	312

<sup>a</sup> Reaction times chosen to avoid gelation. <sup>b</sup> Determined by GPC in THF on the basis of a polystyrene calibration. <sup>c</sup> Glass-transition temperature ( $T_g$ ) of polymers detected by the DSC analyses at a heating rate of 10 °C/min under nitrogen. <sup>d</sup> 5% weight loss temperature of polymers detected by the TGA analyses at a heating rate of 10 °C/min under nitrogen.

Figure 1.  $^1\text{H}$  NMR spectra of hyperbranched polymers **P1–P4** conducted in chloroform-*d*.

physical, optical, and EL properties. **P1–P4** were obtained as brown solid with satisfied yields (Table 1), and they were readily soluble in common organic solvents, such as toluene, THF,  $\text{CHCl}_3$ , and so on.

Figure 1 showed the  $^1\text{H}$  NMR spectra of hyperbranched polymers **P1–P4**, which were conducted in the solvent of chloroform-*d*. All peaks could be readily assigned to the resonances of appropriate protons as demonstrated in Scheme 2, and no unexpected peaks appeared. It was easy to observe the proton peaks at around 7.9 and 8.3 ppm, which were associated with

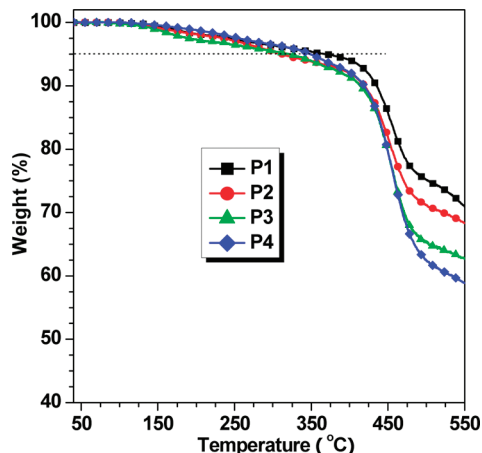


**Figure 2.** TGA curves of polymers measured at a heating rate of 10 °C/min under nitrogen.

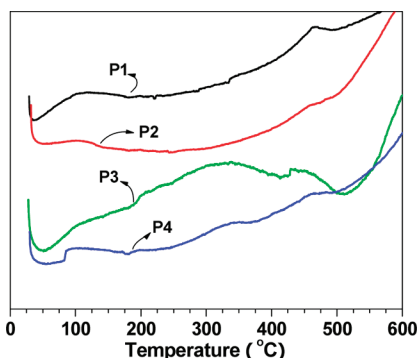


**Figure 3.** DSC curves of polymers measured under nitrogen at a heating rate of 10 °C/min.

the phenyl rings in oxadiazole units, indicating the success of polymerization. The molar ratio of the moieties of **2** and **10** in polymers could be calculated from the integration ratios of the phenyl protons derived from **2** (8.3 ppm) versus the methylene moieties linked to the nine-position of fluorene units (2.0 ppm). The values in **P2**, **P3**, and **P4** were estimated to be 1:3.3, 2:3.8, and 2:3.8, respectively, in which only that of **P4** was very close to the feed one. The difference between the estimated molar percents of **P2** and **P3** and the feed ones should be ascribed to the relatively bad solubility of compound **9**, which could not be dissolved completely at the very beginning of polymerization reaction. Therefore, the percents of compound **9** in **P2** and **P3** were relatively lower than those in feed ones. As shown in Table 1, the number-average ( $M_n$ ) and weight-average molecular weights ( $M_w$ ) of **P1–P4**, determined by gel permeation chromatography (GPC) using THF as solvent and monodisperse polystyrene as calibration standard, were in the range of 12 500–32 100, with polydispersity indexes (PDIs) lying around 1.42 to 3.05, indicating the successful preparation of soluble hyperbranched polymers.

**Thermal Properties.** The thermal behavior of the polymers was investigated by TGA (thermal gravimetric analysis) and DSC (differential scanning calorimetry) under an atmosphere of nitrogen. As shown in Figure 2, the TGA results demonstrated that all polymers (**P1–P4**) exhibited good thermal stability with 5% weight loss temperatures ranging from 312 to 364 °C (Table 1). No crystallization and melting peaks, which usually appeared in PFs,<sup>59</sup> but only glass-transition temperatures ( $T_g$  values) were observed in DSC traces of **P1–P4** (Figure 3) because high branched structure of hyperbranched polymers and the introduced hexaphenylbenzene moieties could efficiently suppress

the crystallization (or chain aggregation) of the polymer chains. The  $T_g$  values of **P1–P4** were in the range of 155 to 191 °C (Table 1), much higher than those of PFs,<sup>59</sup> disclosing the good amorphous properties of these polymers. The relatively high  $T_g$  and  $T_d$  of the hyperbranched polymers would contribute to their OLED applications to a large degree because the lifetime of PLEDs was known to depend critically on the thermal stability of the active polymers.

**Optical Properties.** The optical characteristics of the polymers were investigated both in solutions and as cast thin films. Their absorption and PL spectra in THF and films are shown in Figures 4 and 5, and the related spectral maxima were summarized in Table 2. **P1–P4** demonstrated absorption maxima ( $\lambda_{\max}$ ) around 339–365 nm, both in solution and film, which were attributed to the  $\pi$ – $\pi^*$  transition of the conjugated oligofluorene segments. The absorption maxima in both solutions and films were nearly the same, indicating the inhibition of aggregation in the hyperbranched polymers **P1–P4**. In addition, the  $\lambda_{\max}$  of **P4** (364 nm) was red-shifted about 24 nm compared with that of **P1** (340 nm) because the introduction of oxadiazole units gently enhanced the degree of intramolecular charge transfer. Figure 5A showed the PL emission spectra, and all of the polymers exhibited strong and deep blue light emission upon exciting, and the emitting maxima were around 401–425 nm with narrow fwhm of about 40 nm. Thanks to their special hyperbranched structure, the emission spectra of **P1–P4** in films were nearly the same as those in solutions (Figure 5B), with only a little red shift, unlike the PL spectrum of the PF film, in which there was an aggregation peak around 520 nm besides two excitonic emission peaks. In comparison with the nearly unchanged emission wavelengths of the solid films of **P1** and **P2**, there were some differences for **P3** and **P4**, indicating that there should be some aggregations in the solid states. It was reasonable that in these two polymers the feed ratio of monomer **2** increased; as a result, the linear part in the resultant hyperbranched polymers would increase, which would destroy the hyperbranched structure of the polymers in some degree, thus leading to the observed aggregation phenomena. The PL quantum yields ( $\Phi_F$ ) of **P1–P4** in diluted THF solutions were also measured using 9,10-diphenylanthracene in cyclohexane ( $\Phi_F = 90\%$ ) as reference (Table 1). **P1** demonstrated the lowest quantum yield (0.38), whereas those of **P2–P4** had much higher quantum efficiency yield (0.85 to 0.91) than that of poly(2,7-(9,9-dioctyl)-fluorene)s ( $\Phi_F = 0.78$ ). This might be due the slightly enhanced intramolecular charge transfer as a result of the introduced oxadiazole units.

To investigate the fluorescence stability of the polymers in the solid state, we performed annealing experiments. The solid films of **P1–P4** were first baked at 150 °C for 30 min in air, then at 175 °C for another 30 min, followed by 200 °C. Figure 6 and Figure S1 of the Supporting Information showed the normalized PL emission spectra of the polymers after annealing in air. It was reported that thermal treatment of the film of poly(dihexylfluorene) at 100 °C would lead to a significant increase in the shoulder peak centered at  $\sim 460$  nm because of the aggregation effect or keto formation in air.<sup>60</sup> However, **P1–P4** were very stable after they were baked at 150 °C for 0.5 h, and the PL spectra were almost the same as those tested before annealing. Accompanying the further increased temperature, there appeared a new shoulder peak at  $\sim 510$  nm, which was not apparent after annealing at 175 °C for another 0.5 h, clearly suggesting that hyperbranched structure resulted in better spectra–thermal stability, and the formation of aggregation

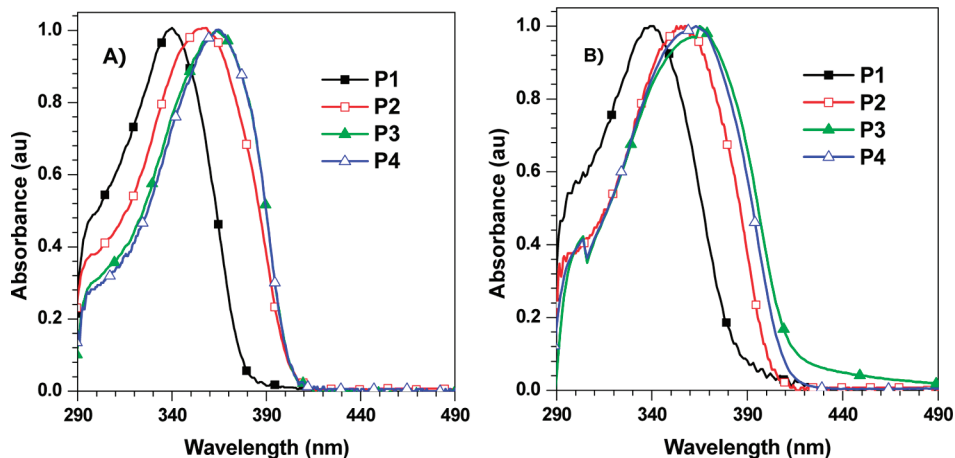


Figure 4. UV-vis spectra of polymers **P1**–**P4** in THF solutions (A) and in films (B).

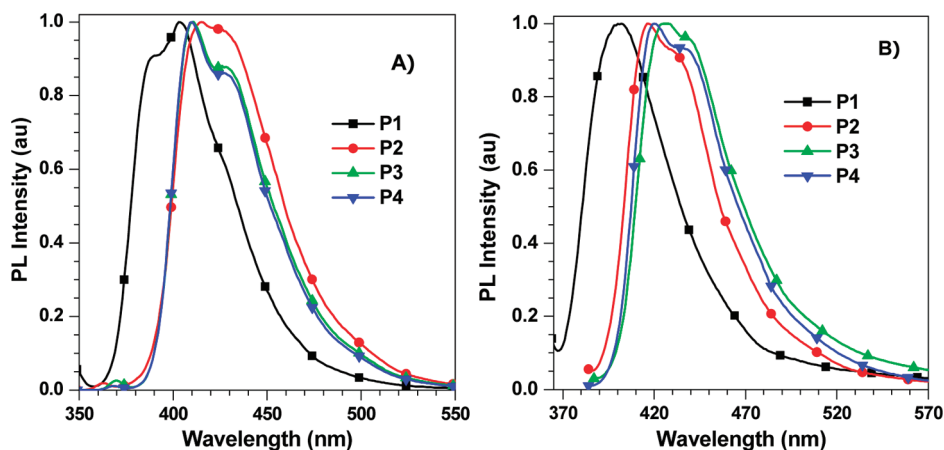


Figure 5. PL spectra of polymers **P1**–**P4** in THF solutions (A) and in films (B).

TABLE 2: Optical Properties of Polymers in Solution and Solid State

no.	$\lambda_{\text{abs,sol}}^a$ (nm)	$\lambda_{\text{PL,sol}}^a$ (nm)	$\lambda_{\text{abs,film}}^b$ (nm)	$\lambda_{\text{PL,film}}^b$ (nm)	$\Phi_F^c$
<b>P1</b>	340	403	339	401	0.38
<b>P2</b>	356	415	356	417	0.85
<b>P3</b>	364	410	365	425	0.86
<b>P4</b>	364	410	363	420	0.91

<sup>a</sup> Absorption wavelength of polymer solutions in THF; the concentration was  $2 \times 10^{-3}$  mg/mL. <sup>b</sup> Emission wavelength of polymer in films. <sup>c</sup> Quantum yields in THF solutions using 9,10-diphenylanthracene in cyclohexane ( $\Phi_F = 90\%$ ) as standard.

excimer and keto defects in these hyperbranched polymers were effectively suppressed.<sup>29–38</sup>

**Electrochemical Characterization.** The electrochemical properties of the polymers were investigated by using cyclic voltammetry (CV), and their scanned cyclic voltammograms were shown in Figure 7, with the electrochemical data summarized in Table 3. The onset oxidation potentials of hyperbranched polymers **P1**–**P4** occurred at around 0.96 to 1.06 V, whereas the onset reduction potentials occurred at about −2.25 to −2.43 V. On the basis of these onset potentials and according to the equations of  $E_{\text{HOMO}} = -(E_{\text{onset(ox),FOC}} + 4.8)$  eV and  $E_{\text{LUMO}} = -(E_{\text{onset(red),FOC}} + 4.8)$  eV, the HOMO and LUMO energy levels of the polymers could be estimated (Table 3). It was easily seen that the HOMO energy of polymers decreased slightly with increasing content of oxadiazole units, but all of which were in the range of 5.76 to 5.86 eV, similar to that of poly(9,9-

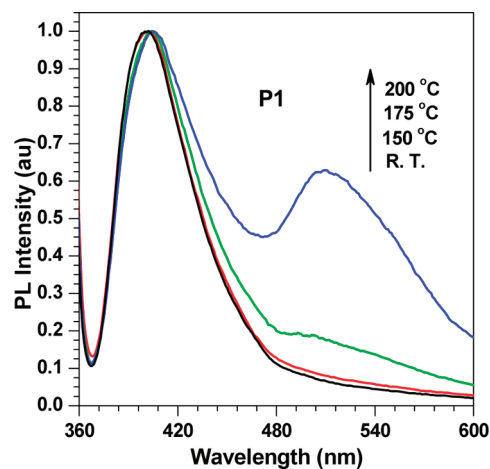


Figure 6. Photoluminescence spectra of the films of **P1** before and after annealing at different temperatures for 30 min in air.

diocylfluorene) (POF) (5.80 eV), meaning that these polymers possessed hole-transporting ability in some degree. In addition, these polymers also exhibited low LUMO energy level in the range of −2.37 to −2.58 eV, indicating the easier electron injection, and the oxadiazole units would act as the electron transport agents in the polymers. Therefore, the charge transporting in these hyperbranched polymers constructed by the electron- and hole-transporting segments might be balanced.

**Electroluminescence Properties.** To study the electroluminescent properties of **P1**–**P4**, we fabricated double-layer devices (ITO/PEDOT/**P1**–**P4**/TPBI/Ca/Ag) using these polymers as the



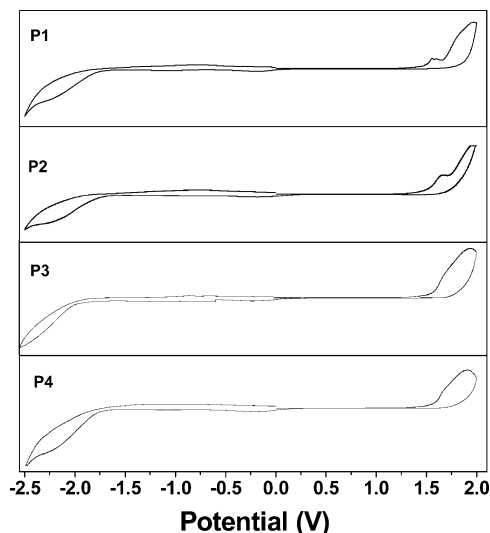


Figure 7. Cyclic voltammograms of the polymers films on Pt working electrode.

TABLE 3: Electrochemical Properties of Polymers

no.	$E_g^{\text{opt}}$	$E_{\text{onset(ox)}}$	$E_{\text{HOMO}}$	$E_{\text{onset(red)}}$	$E_{\text{LUMO}}$	$E_g^e$
no.	(eV) <sup>a</sup>	(V) vs FOC <sup>b</sup>	(eV) <sup>c</sup>	(V) vs FOC <sup>b</sup>	(eV) <sup>d</sup>	(eV) <sup>d</sup>
P1	3.24	0.96	-5.76	-2.25	-2.55	-3.21
P2	3.09	0.99	-5.79	-2.22	-2.58	-3.21
P3	3.02	1.04	-5.84	-2.43	-2.37	-3.47
P4	3.01	1.06	-5.86	-2.25	-2.55	-3.31

<sup>a</sup> Band gaps obtained from absorption edge ( $E_g = 1240/\lambda_{\text{onset}}$ ).

<sup>b</sup>  $E_{\text{FOC}} = 0.48$  V versus Ag/AgCl. <sup>c</sup>  $E_{\text{HOMO}} = -(E_{\text{onset(ox),FOC}} + 4.8)$  eV. <sup>d</sup>  $E_{\text{LUMO}} = -(E_{\text{onset(red),FOC}} + 4.8)$  eV. <sup>e</sup>  $E_g = \text{LUMO} - \text{HOMO}$ .

TABLE 4: EL Data of PLEDs Devices

no.	$V_{\text{on}}^a$	$\text{lumin}^b$	$\text{CD}^c$	$\text{CE}^d$
no.	(V)	$L$ (cd/m <sup>2</sup> )	$J$ (mA/cm <sup>2</sup> )	(cd/A)
P1	12.0	251(30.5)	427	0.46
P2	10.5	221(22.0)	365	0.48
P3	6.0	549(16.5)	358	0.72
P4	7.5	552(17.5)	405	0.63

<sup>a</sup> Turn-on voltage. <sup>b</sup> Maximum luminescence; the corresponding operating voltage is given in the parentheses. <sup>c</sup> Current density at the maximum luminescence, also the maximum current density. <sup>d</sup> Maximum luminescence efficiency.

emitting layers, with their EL data of PLED devices shown in Table 4. When a bias potential was applied to the electrodes, the deeply blue EL emissions centered at  $\sim 420$  nm could be achieved from the EL devices of **P1–P4** (Figure 8), indicating that the intermolecular interactions of the polymer were very weak, thanks to the hyperbranched structure. The EL spectra were very narrow with fwhm values of  $\sim 40$  nm, which corresponded well with their PL curves, showing that the obtained blue emission was very pure. This was reasonable. According to our previous experimental results, the multisubstituted arylated benzene derivatives would be aggregation-induced emission (AIE) or aggregation-induced emission enhancement (AIEE) molecules,<sup>61</sup> which meant, in solid state, in comparison with those in solutions, the fluorescence of these molecules would not be quenched but enhanced. Here in the hyperbranched polymers **P1–P4**, the used hexaphenylbenzene core would contribute much to the suppression of the formation of aggregation excimers in the solid state, just like other multisubstituted arylated benzene derivatives previously reported, in addition to the contribution from the internal

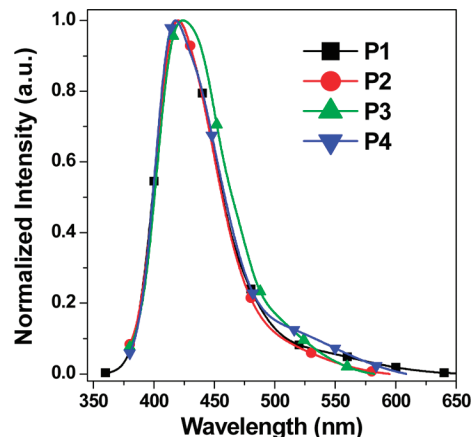


Figure 8. EL spectra of hyperbranched polymers **P1–P4**.

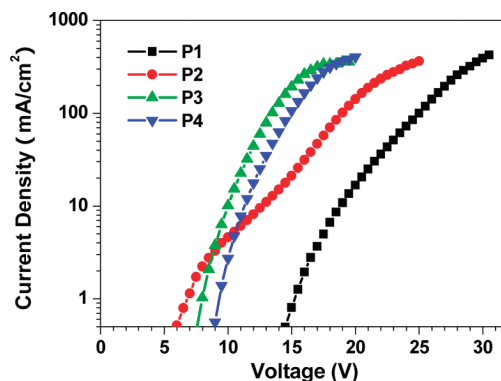


Figure 9. Current–voltage characteristics of the PLEDs devices.

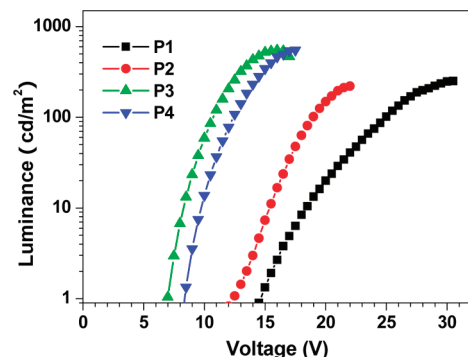
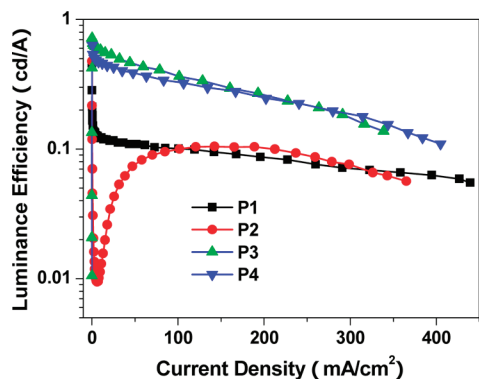


Figure 10. Luminescence–voltage characteristics of the PLEDs devices.

hyperbranched structure. Also, as discussed above, the spectra–thermal stability of these hyperbranched polymers was much better than that reported for poly(dihexylfluorene). This point would surely benefit the long-term stability of the LED performance in the practical applications.

The voltage–luminescence and voltage–current density characteristics of these two devices are shown in Figures 9 and 10. **P1** demonstrated relatively good EL performance compared with most “A<sub>3</sub>+B<sub>2</sub>”-type hyperbranched polymers, with the maximum current density and luminescence up to 427 mA/cm<sup>2</sup> and 251 cd/m<sup>2</sup>, respectively, which might be attributed to the 2D structure of hexaphenylbenzene moieties used as the core for hyperbranched polymers. However, the turn-on voltage of **P1**-based device (12 V) was relatively high. Fortunately, by the introduction of oxadiazole units, the turn-on voltage decreased (Table 4), and the turn-on voltage of **P3**-based device was only 6 V, much lower than that of **P1**, because oxadiazole units were



**Figure 11.** Luminescence efficiency–current characteristics of PLEDs devices.

electron-deficient groups, leading to the very efficient transport of electronic charges.<sup>46–49</sup> In addition, the maximum luminescence of **P3** and **P4**, as high as 550 cd/m<sup>2</sup>, increased dramatically in comparison with that of **P1**, although the current density decreased a little. Figure 11 displayed the luminescence efficiency–current characteristics of PLEDs devices of polymers, and **P3** and **P4** exhibited much higher luminescence efficiency (0.72 and 0.63, respectively) than that of **P1** (0.48). These results suggested that the incorporation of electron-transporting oxadiazole units was effective in improving EL performance of the devices, confirming our original idea. **P2** showed similar EL performance as **P1** because of its relatively lower percent of oxadiazole units in comparison with those of **P3** and **P4**, indicating the importance of oxadiazole units on another side. Also, by adjusting the feeding ratios of the monomers, especially the content of oxadiazole units, the performance of the resultant hyperbranched polymers could be modified accordingly. Anyhow, the EL results of all polymers, especially **P3**, were relatively good for hyperbranched polymers, and these preliminary data demonstrated the applicability of these novel hyperbranched polymers as stable and high-efficient PLED blue-emitters thanks to their special structure. It should be pointed out that the EL devices of these hyperbranched polymers were not optimized, and thus better performance might be achieved.

## Conclusions

In this article, for the first time, a new series of hexaphenylbenzene- and oxadiazole-based hyperbranched conjugated polymers (**P1–P4**) was prepared successfully by an “A<sub>3</sub>+B<sub>2</sub>+C<sub>2</sub>” approach through one-pot Suzuki polycondensation reaction. All polymers exhibited good thermal stabilities (*T*<sub>d</sub> > 310 °C and *T*<sub>g</sub> > 155 °C) and bright deep blue emission in both solutions and solid state. The deep blue light emission of their films was very pure and stable, and no long wavelength excimer-like emissions at 500–600 nm derived from self-aggregation of PFs in the solid state were observed in their spectra, even after annealing at 150 °C for 0.5 h, indicating that the hyperbranched structure and the introduced hexaphenylbenzene moieties effectively suppressed the formation of aggregation excimer and keto defects. Two-layer PLED devices (ITO/PEDOT/**P1–P4**/TPBI/Ca/Ag) have been fabricated, and their electroluminescence properties were investigated. These polymers demonstrated relatively good EL performance, and the **P1**-based device showed a maximum luminescence of 251 cd/m<sup>2</sup>, with the maximum luminescence efficiency of 0.46. Owing to the introduced electron-transporting groups, oxadiazole units, the EL performance of **P3** and **P4** was improved dramatically, with

the maximum luminescence of ~550 cd/m<sup>2</sup> and the maximum luminescence efficiency as high as 0.72 cd/A.

## Experimental Section

**Materials and Instrumentation.** Tetrahydrofuran (THF) was dried over and distilled from K–Na alloy under an atmosphere of dry nitrogen. Triethylamine (Et<sub>3</sub>N) was distilled under normal pressure and kept over potassium hydroxide. All other reagents were used as received.

The <sup>1</sup>H NMR and <sup>13</sup>C NMR spectra were measured on a Varian Mercury300 spectrometer or Bruker ARX 400 spectrometer using tetramethylsilane (TMS; δ 0) as internal standard. UV–visible spectra were obtained using a Shimadzu UV-2551 spectrometer. PL spectra were recorded on a Hitachi F-4500 fluorescence spectrophotometer. GPC was used to determine the molecular weights of polymers. GPC analysis was performed on an Agilent 1100 series HPLC system and a G1362A refractive index detector. Polystyrene standards were used as calibration standards for GPC. THF was used as an eluent, and the flow rate was 1.0 mL/min. Elemental analyses were performed by a CARLOERBA-1106 microelemental analyzer. Thermal analysis was performed on a NETZSCH STA449C thermal analyzer at a heating rate of 10 °C/min in nitrogen at a flow rate of 50 cm<sup>3</sup>/min for thermogravimetric analysis (TGA). The thermal transitions of the polymers were investigated using a Mettler differential scanning calorimeter DSC822e under nitrogen at a scanning rate of 10 °C/min. CV was carried out on a CHI voltammetric analyzer in a three-electrode cell with a Pt counter electrode, a Ag/AgCl reference electrode, and a glassy carbon working electrode at a scan rate of 10 mV s<sup>−1</sup> with 0.1 M tetrabutylammonium perchlorate (purchased from Alfa Aesar) as the supporting electrolyte in anhydrous acetonitrile solution purged with nitrogen. The potential values obtained in reference to the Ag/Ag<sup>+</sup> electrode were converted to values versus the saturated calomel electrode (SCE) by means of an internal ferrocenium/ferrocene (Fc<sup>+</sup>/Fc) standard.

**1,2,4-Tri(4-bromophenyl)-3,5,6-triphenylbenzene (9).** A mixture of 3,4-bis(4-bromophenyl)-2,5-diphenyl-2,4-cyclopentadien-1-one (**8**) (0.54 g, 1.00 mmol) and 1-bromo-4-(phenylethynyl)benzene (**5**) (0.25 g, 0.97 mmol) in diphenyl ether (2 mL) was heated at reflux under nitrogen for 2 days. The resultant mixture was cooled to room temperature and then diluted with ethanol. The precipitate was collected by filtration, washed with ethanol and hexane, and dried to give compound **9** as a nearly colorless solid (0.64 g, 85.8%). <sup>1</sup>H NMR (300 MHz, CDCl<sub>3</sub>, 298 K, δ): 6.65 (d, *J* = 7.8 Hz, 6H, ArH), 6.77 (br, s, 6H, ArH), 6.90 (m, 9H, ArH), 7.00 (m, 6H, ArH). <sup>13</sup>C NMR (100 MHz, CDCl<sub>3</sub>, 298 K, δ): 119.61, 118.81, 125.62, 125.80, 126.90, 127.10, 129.87, 130.08, 131.15, 132.84, 139.18, 139.30, 139.85, 140.60. C<sub>42</sub>H<sub>27</sub>Br<sub>3</sub> (EA) (%), found/calcd): C, 64.71/65.40; H, 3.45/3.53.

**General Synthetic Procedure for Hyperbranched Polymer P1–P4.** To a solution of predetermined amount of monomers (**2**, **9**, and **10**), sodium carbonate (10 equiv of **10**) and a catalytic amount of tetrakis(triphenylphosphine) palladium (Pd(PPh<sub>3</sub>)<sub>4</sub>) (1–3.0 mol %) were added; the resultant mixture in THF (the concentration of **10** was controlled at 0.025 mol/L)/H<sub>2</sub>O (4/1, v/v) was carefully degassed and exchanged with nitrogen three times. The solution was then stirred at 65 °C under nitrogen. Before gelation, the end groups were then capped by refluxing 3–8 h each time with phenylboronic acid and bromobenzene sequentially. Excess methanol was poured in the mixture, which was then filtered. The obtained solid was dissolved in THF, and the insoluble solid was filtered out. After removal of the

solvent, the residue was further purified by several precipitations from THF into acetone; then, the obtained solid was collected by filtration and dried under vacuum.

**P1.** **9** (77 mg, 0.10 mmol), **10** (75 mg, 0.15 mmol). **P1** was obtained as yellow solid (65 mg, 63.1%).  $M_w = 12\,500$ ,  $M_w/M_n = 1.70$ , (GPC, polystyrene calibration).  $^1\text{H}$  NMR (400 MHz,  $\text{CDCl}_3$ , 298 K,  $\delta$ ): 0.5–0.8 ( $-\text{CH}_3$ ), 1.0–1.2 ( $-\text{CH}_2-$ ), 1.8–2.0 ( $-\text{CH}_2\text{C}-$ ), 6.8–7.1 (ArH), 7.1–7.5 (ArH), 7.6–7.7 (ArH).

**P2.** **9** (70 mg, 0.09 mmol), **2** (17 mg, 0.045 mmol), **10** (90 mg, 0.18 mmol). **P2** was obtained as brown solid (82 mg, 69.3%).  $M_w = 32\,100$ ,  $M_w/M_n = 2.35$ , (GPC, polystyrene calibration).  $^1\text{H}$  NMR (400 MHz,  $\text{CDCl}_3$ , 298 K,  $\delta$ ): 0.5–0.9 ( $-\text{CH}_3$ ), 1.0–1.2 ( $-\text{CH}_2-$ ), 1.8–2.2 ( $-\text{CH}_2\text{C}-$ ), 6.7–7.1 (ArH), 7.2–7.3 (ArH), 7.3–7.5 (ArH), 7.6–7.8 (ArH), 7.9 (ArH), 8.3 (ArH).

**P3.** **9** (46 mg, 0.06 mmol), **2** (23 mg, 0.06 mmol), **10** (75 mg, 0.15 mmol). **P3** was obtained as brown solid (69 mg, 70.9%).  $M_w = 12\,500$ ,  $M_w/M_n = 1.42$ , (GPC, polystyrene calibration).  $^1\text{H}$  NMR (400 MHz,  $\text{CDCl}_3$ , 298 K,  $\delta$ ): 0.6–0.9 ( $-\text{CH}_3$ ), 1.0–1.2 ( $-\text{CH}_2-$ ), 1.9–2.2 ( $-\text{CH}_2\text{C}-$ ), 6.7–7.1 (ArH), 7.3–7.6 (ArH), 7.6–7.8 (ArH), 7.8–8.0 (ArH), 8.3 (ArH).

**P4.** **9** (46 mg, 0.06 mmol), **2** (46 mg, 0.12 mmol), **10** (106 mg, 0.21 mmol). **P4** was obtained as brown solid (82 mg, 80.7%).  $M_w = 20\,300$ ,  $M_w/M_n = 3.05$ , (GPC, polystyrene calibration).  $^1\text{H}$  NMR (400 MHz,  $\text{CDCl}_3$ , 298 K,  $\delta$ ): 0.6–0.9 ( $-\text{CH}_3$ ), 1.0–1.3 ( $-\text{CH}_2-$ ), 1.9–2.2 ( $-\text{CH}_2\text{C}-$ ), 6.7–7.1 (ArH), 7.2–7.6 (ArH), 7.6–7.8 (ArH), 7.8–8.0 (ArH), 8.3 (ArH).

**Fabrication and Characterization of OLEDs.** In a general procedure, indium–tin oxide (ITO)-coated glass substrates were etched, patterned, and washed with detergent, deionized water, acetone, and ethanol sequentially. We fabricated OLEDs using polymers **P1–P4** as the emissive layer with a structure of ITO/PEDT–PSS/**P1–P4**/TPBI/cathode, where the polyethylene dioxythiophene–polystyrene sulfonate (PEDT–PSS) and 2,2',2''-(1,3,5-benzenetriyl)tris[1-phenyl-1H-benzimidazole] (TPBI) were used as hole injection and hole-blocking/electron-transporting layer, respectively. The active layer was spin-coated from chloroform solution, and TPBI layer was deposited by means of conventional vacuum deposition onto the ITO-coated glass substrates at a pressure of  $8 \times 10^{-5}$  Pa. In all devices, a cathode Ca/Ag layer with the weight ration of 10:1 and a 100-nm-thick Ag capping layer were deposited through a 2-mm-diameter opening in a shadow mask. The active area of device was 5 mm<sup>2</sup>. A quartz crystal oscillator placed near the substrate was used to monitor the thickness of each layer, which was calibrated ex situ using an Ambios Technology XP-2 surface profilometer. UV–vis absorption and fluorescence spectra were collected with a Hitachi U-3010 and Hitachi F-4500 spectrophotometer, respectively. EL spectra and chromaticity coordinates were measured with a SpectraScan PR650 photometer. Current density–voltage–luminance ( $J$ – $V$ – $L$ ) measurements were made simultaneously using a Keithley 4200 semiconductor parameter analyzer and a Newport multifunction 2835-C optical meter, and luminance was measured in the forward direction. All device characterizations were carried out under ambient laboratory air at room temperature.

**Acknowledgment.** We are grateful to the National Science Foundation of China (nos. 20974084, 20825208, 60736004), the Program for NCET, and Fundamental Research Funds for the Central Universities (no. 5081002) for financial support.

**Supporting Information Available:** Synthetic procedure for compounds **2**, **5**, and **8**. PL spectra of the films of **P2–P4** before and after annealing at different temperatures for 30 min in air. This material is available free of charge via the Internet at <http://pubs.acs.org>.

## References and Notes

- (1) Burroughes, J. H.; Bradley, D. D. C.; Brown, A. R.; Marks, R. N.; Mackay, K.; Friend, R. H.; Burn, P. L.; Holmes, A. B. *Nature* **1990**, *347*, 539.
- (2) Jenekhe, S. A. *Adv. Mater.* **1995**, *7*, 309.
- (3) Hide, F.; Diaz-Garcia, M. A.; Schartz, B. J.; Heeger, A. J. *Acc. Chem. Res.* **1997**, *30*, 430.
- (4) Müller, C. D.; Falcou, A.; Reckefuss, N.; Rojahn, M.; Wiederhorn, V.; Rudati, P.; Frohne, H.; Nuyken, O.; Becker, H.; Meerholz, K. *Nature* **2003**, *421*, 829.
- (5) Friend, R. H.; Gymer, R. W.; Holmes, A. B.; Burroughes, J. H.; Marks, R. N.; Taliani, C.; Bradley, D. D. C.; Dos Santos, D. A.; Bredas, J. L.; Lögglund, M.; Salaneck, W. R. *Nature* **1999**, *397*, 121.
- (6) Kim, D. Y.; Cho, H. N.; Kim, C. Y. *Prog. Polym. Sci.* **2000**, *25*, 1089.
- (7) Pei, Q. B.; Yang, Y. J. *Am. Chem. Soc.* **1996**, *118*, 7416.
- (8) Bemius, M. T.; Mike, I.; O'Brien, J.; Wu, W. *Adv. Mater.* **2000**, *12*, 1737.
- (9) Scherf, U.; List, E. J. W. *Adv. Mater.* **2002**, *14*, 477.
- (10) Kraft, A.; Grimsdale, A. C.; Holmes, A. B. *Angew. Chem., Int. Ed.* **1998**, *37*, 402.
- (11) Yang, R. Q.; Tian, R. Y.; Hou, Q.; Yang, W.; Cao, Y. *Macromolecules* **2003**, *36*, 7453.
- (12) Leclerc, M. *J. Polym. Sci., Part A: Polym. Chem.* **2001**, *22*, 1365.
- (13) (a) Jenekhe, S. A.; Osaheni, J. A. *Science* **1994**, *265*, 765. (b) Chan, K. L.; Sims, M.; Pascu, S. I.; Ariu, M.; Holmes, A. B.; Bradley, D. D. C. *Adv. Funct. Mater.* **2009**, *13*, 2147.
- (14) (a) Gong, X.; Iyer, P. K.; Moses, D.; Bazan, G. C.; Heeger, A. J.; Xiao, S. S. *Adv. Funct. Mater.* **2003**, *13*, 325. (b) Tseng, S.; Li, S.; Meng, H.; Yu, Y.; Yang, C.; Liao, H.; Horng, S.; Hsu, C. *Org. Electron.* **2008**, *9*, 279.
- (15) List, E. J. W.; Guentner, R.; Scandiucci de Freitas, P.; Scherf, U. *Adv. Mater.* **2002**, *14*, 374.
- (16) Klärner, G.; Davey, M. H.; Chen, W. D.; Scott, J. C.; Miller, R. D. *Adv. Mater.* **1998**, *10*, 993.
- (17) Craig, M. R.; de Kok, M. M.; Hofstra, J. W.; Schenning, A. P. H. J.; Meijer, E. W. *J. Mater. Chem.* **2003**, *13*, 2861.
- (18) Romaner, L.; Pogantsch, A.; De Freitas, P. S.; Scherf, U.; Gaal, M.; Zojer, E.; List, E. J. W. *Adv. Funct. Mater.* **2003**, *13*, 597.
- (19) Halim, M.; Samuel, I. D. W.; Pillow, J. N. G.; Bourn, P. L. *Synth. Met.* **1999**, *102*, 1113.
- (20) Satoh, N.; Cho, J. S.; Higuchi, M.; Yamamoto, K. *J. Am. Chem. Soc.* **2003**, *125*, 8104.
- (21) Kimoto, A.; Cho, J.-S.; Higuchi, M.; Yamamoto, K. *Macromolecules* **2004**, *37*, 5531.
- (22) Furuta, P.; Brooks, J.; Thompson, M. E.; Fréchet, J. M. J. *J. Am. Chem. Soc.* **2003**, *125*, 13165.
- (23) Pogantsch, A.; Wenzl, F. P.; List, E. J. W.; Leising, G.; Grimsdale, A. C.; Müllen, K. *Adv. Mater.* **2002**, *12*, 1061.
- (24) Jiang, Y.; Wang, L.; Zhou, Y.; Cui, Y.-X.; Wang, J.; Cao, Y.; Pei, J. *Chem. Asian J.* **2009**, *4*, 548.
- (25) Lo, S.-C.; Burn, P. L. *Chem. Rev.* **2007**, *107*, 1097.
- (26) Häußler, M.; Tang, B. Z. *Adv. Polym. Sci.* **2007**, *209*, 1.
- (27) Kim, Y. H. *J. Polym. Sci., Part A: Polym. Chem.* **1998**, *36*, 1685.
- (28) Sunder, A.; Heinemann, J.; Frey, H. *Chem.–Eur. J.* **2000**, *6*, 2499.
- (29) Li, J.; Bo, Z. *Macromolecules* **2004**, *37*, 2013.
- (30) Ding, L.; Bo, Z.; Chu, Q.; Li, J.; Dai, L.; Pang, Y. *Macromol. Chem. Phys.* **2006**, *207*, 870.
- (31) Sun, M.; Li, J.; Li, B.; Fu, Y.; Bo, Z. *Macromolecules* **2005**, *38*, 2651.
- (32) He, Q.-Y.; Lai, W.-Y.; Ma, Z.; Chen, D.-Y.; Huang, W. *Eur. Polym. J.* **2008**, *44*, 3169.
- (33) Tang, D.; Wen, G.; Qi, X.; Wang, H.; Peng, B.; Wei, W.; Huang, W. *Polymer* **2007**, *48*, 4412.
- (34) Liu, X.; Lin, T.; Huang, J.; Hao, X.; Ong, K. S.; He, C. *Macromolecules* **2005**, *38*, 4157.
- (35) Liu, X.; Xu, J.; Lu, X.; He, C. *Org. Lett.* **2005**, *7*, 2829.
- (36) Wu, C.-W.; Lin, H.-C. *Macromolecules* **2006**, *39*, 7232.
- (37) Tsai, L.-R.; Chen, Y. *Macromolecules* **2007**, *40*, 2984.
- (38) Tsai, L.-R.; Chen, Y. *Macromolecules* **2008**, *41*, 5098.
- (39) Berresheim, A. J.; Müller, M.; Müllen, K. *Chem. Rev.* **1999**, *99*, 1747.
- (40) Keegstra, M. A.; De Feyter, S.; De Schryver, F. C.; Müllen, K. *Angew. Chem., Int. Ed. Engl.* **1996**, *35*, 774.

- (41) Setayesh, S.; Grimsdale, A. C.; Weil, T.; Enkelmann, V.; Müllen, K.; Meghdadi, F.; List, E. J. W.; Leising, G. *J. Am. Chem. Soc.* **2001**, *123*, 946.
- (42) Englert, B. C.; Smith, M. D.; Hardcastle, K. I.; Bunz, U. H. F. *Macromolecules* **2004**, *37*, 8212.
- (43) Dinakaran, K.; Hsiao, S.-M.; Chou, C.-H.; Shu, S.-L.; Wei, K.-H. *Macromolecules* **2005**, *38*, 10429.
- (44) Strukelj, M.; Papadimitrakopoulos, F.; Miller, M. T.; Rothberg, L. J. *Science* **1995**, *267*, 1969.
- (45) Tong, Q.-X.; Lai, S.-L.; Chan, M.-Y.; Lai, K.-H.; Tang, J.-X.; Kwong, H.-L.; Lee, C.-S.; Lee, S.-T. *Chem. Mater.* **2007**, *19*, 5851.
- (46) Hughes, G.; Bryce, M. R. *J. Mater. Chem.* **2005**, *15*, 94.
- (47) (a) Chen, S.-H.; Chen, Y. *Macromolecules* **2005**, *38*, 53. (b) Yu, W. L.; Meng, H.; Pei, J.; Huang, W.; Li, Y.; Heeger, A. J. *Macromolecules* **1998**, *31*, 4838.
- (48) Zhan, X.; Liu, Y.; Wu, X.; Wang, S.; Zhu, D. *Macromolecules* **2002**, *35*, 2529.
- (49) Mikroyannidis, J. A.; Gibbons, K. M.; Kulkarni, A. P.; Jenekhe, S. A. *Macromolecules* **2008**, *41*, 663.
- (50) (a) Itami, K.; Yamazaki, D.; Yoshida, J. *J. Am. Chem. Soc.* **2004**, *126*, 15396. (b) Wang, C.; Jung, G.; Batsanov, A. S.; Bryce, M. R.; Petty, M. C. *J. Mater. Chem.* **2002**, *12*, 173.
- (51) Yasuda, T.; Imase, T.; Nakamura, Y.; Yamamoto, T. *Macromolecules* **2005**, *38*, 4687.
- (52) Wen, G.-A.; Xin, Y.; Zhu, X.-R.; Zeng, W.-J.; Zhu, R.; Feng, J.-C.; Cao, Y.; Zhao, L.; Wang, L.-H.; Wei, W.; Peng, B.; Huang, W. *Polymer* **2007**, *48*, 1824.
- (53) Ma, Z.; Lu, S.; Fan, Q.-L.; Qing, C.-Y.; Wang, Y.-Y.; Wang, P.; Huang, W. *Polymer* **2006**, *47*, 7382.
- (54) Xin, Y.; Wen, G.; Zeng, W.; Zhao, L.; Zhu, X.; Fan, Q.; Feng, J.; Wang, L.; Wei, W.; Peng, B.; Cao, Y.; Huang, W. *Macromolecules* **2005**, *38*, 6755.
- (55) Wu, G.; Yang, Y.; He, C.; Chen, X.; Li, Y. *Eur. Polym. J.* **2008**, *44*, 4047.
- (56) Maly, K. E.; Gagnon, E.; Maris, T.; Wuest, J. D. *J. Am. Chem. Soc.* **2007**, *129*, 4306.
- (57) Li, Z.; Di, C.; Zhu, Z.; Yu, G.; Li, Z.; Zeng, Q.; Li, Q.; Liu, Y.; Qin, J. *Polymer* **2006**, *47*, 7889.
- (58) Li, Z.; Liu, Y.; Yu, G.; Wen, Y.; Guo, Y.; Ji, L.; Qin, J.; Li, Z. *Adv. Funct. Mater.* **2009**, *19*, 2677.
- (59) Grell, M.; Bradley, D. D. C.; Inbasekaran, M.; Woo, E. P. *Adv. Mater.* **1997**, *9*, 798.
- (60) Sims, M.; Bradley, D. D. C.; Ariu, M.; Koeberg, M.; Asimakis, A.; Grell, M.; Lidzey, D. G. *Adv. Funct. Mater.* **2004**, *14*, 765.
- (61) Zeng, Q.; Li, Z.; Dong, Y.; Di, C.; Qin, A.; Hong, Y.; Zhu, Z.; Jim, C. K. W.; Yu, G.; Li, Q.; Li, Z.; Liu, Y.; Qin, J.; Tang, B. *Z. Chem. Commun.* **2007**, 70.

JP1014077